THE JOURNAL OF PHYSICAL CHEMISTRY B LETTERS

**2005,** *109,* 17771−17774
Published on Web 08/31/2005



# Molecular Structure and OH-Stretch Spectra of Liquid Water Surface

**V. Buch**

*The Fritz Haber Institute for Molecular Dynamics, The Hebrew University, Jerusalem 91904, Israel*

*Received: May 27, 2005; In Final Form: August 2, 2005*

Molecular dynamics simulations are used to investigate typical coordination shells of molecules in the liquid water surface, for two potential energy surfaces. The major undercoordinated species found in the surface include three-coordinated $H_2O$ with either a dangling-H or a dangling-O atom and two-coordinated $H_2O$ with one hydrogen bond via H, and another via O. Vibrational signatures of the different coordinations are calculated. The 3400 $cm^{-1}$ band in the surface sum frequency generation (SFG) spectrum is assigned to four-coordinated molecules within the surface layer. The low-frequency wing of the OH-stretch band, near 3200 $cm^{-1}$ in the SFG spectrum, is proposed to be due to collective excitations of a relatively small number of intermolecularly coupled O−H bond vibrations.

Recently, much theoretical and experimental effort has been devoted to probing the molecular structure of liquid water, with and without solutes. Experimental investigations included sum frequency generation (SFG) and second harmonic generation (SHG) studies, and near-edge X-ray spectroscopy studies, while theoretical studies incorporated molecular dynamics and calculations of vibrational spectra (see, e.g., refs 1−12, and references therein). In particular, striking results were obtained on the molecular specificity of solute interactions with the water surface.[11,12] There has been ongoing discussion on the type of molecular configurations which can be found in the water surface and their spectroscopic signatures.

In this letter, the molecular structure of the neat water surface is discussed from the point of view of the coordination shells of constituent water molecules and the corresponding OH-stretch frequencies. The major coordination types are identified, and their spectroscopic signatures are explored.

**Molecular Dynamics (MD): Technical Details.** Simulations were carried out for a slab of liquid water, with two-dimensional periodic boundaries. Two potential energy surfaces (PES) were employed. The first nonpolarizable potential, TIP4P,[13] was shown to provide a remarkably good qualitative description of the water phase diagram[14] and of liquid water. One may however worry about possible polarization effects in the asymmetric surface environment. Therefore, complementary calculations were carried out with the polarizable EMP potential, which was shown to reproduce quite well the properties of liquid water, ice Ih, and water clusters.[15,16] Molecules were treated as rigid, with the help of the SHAKE algorithm.[17] Potential cutoffs of 11 and 9 Å were employed with TIP4P and EMP, respectively. At this stage, no effort was made to include long-range potential effects, since the latter are unlikely to affect short-range properties such as coordination shells.[18−20] In the case of EMP, the liquid slab of thickness ∼38 Å included 600 water molecules; the slab was prepared by melting 10 layers of ice Ih, of 60 molecules each. In the case of TIP4P, the liquid slab was ∼76 Å thick and included 1200 molecules. Runs of lengths ranging 400−900 ps were used to equilibrate the system; the ensuing 100 ps production run was used to collect the data on the surface structure. On the basis of radial distribution functions, a pair of molecules was defined as hydrogen-bonded if the minimal O···H distance was smaller than 2.35 Å.

**Coordinations of Surface Molecules: MD Results.** The results are summarized in Table 1. The major species of undercoordinated molecules found in the surface layer include two species of three-coordinated $H_2O$: the ones with dangling-O-atom (OHH, 21−23%) and the ones with dangling-H (OOH, 14−17%). In addition, there is a significant contribution from a *single* species of two-coordinated $H_2O$—with one bond via H and another via O (OH, 9−20%). The other possible species of two-coordinated molecules (with two bonds via H or two bonds via O) and singly coordinated $H_2O$ were observed at the level of 2% or less. Relating the computational results to experimental reality is somewhat complicated by the question of whether one should take the room temperature as 298 K or as 25 K above the melting points for each PES (which are 221 K and ∼240 K, respectively, for TIP4P and EMP; see Table 1 footnote). However, the above qualitative results appear quite consistent for all temperatures examined. The abundance of three-coordinated species is constant within a few percent, while the abundance of the two-coordinated OH species varies by only a factor of 2 on the scale of ∼100 K (222−330 K, TIP4P). Moreover, these results are consistent with the ones obtained computationally and experimentally in the past, for low-temperature amorphous ice condensates.[21,22] Similar undercoordinated species can be found in annealed amorphous ice surfaces[21−23] and in surfaces of ice nanocrystals;[24] however, there the percentage of two-coordinated molecules is much smaller. In a perfect crystalline ice Ih surface (1000), only three coordinated species are present.[25,26] However, there is computational evidence for surface reconstruction of crystal ice surfaces upon heating to a disordered structure resembling annealed amorphous ice.[25,26]

10.1021/jp052819a CCC: $30.25 

**TABLE 1: Percentage of Different Hydrogen Bond Coordinations in the Liquid Surface and Subsurface Layers[a]**

| PES[b] | EMP | | EMP | | TIP4P | | TIP4P | | TIP4P | | TIP4P | |
|---|---|---|---|---|---|---|---|---|---|---|---|---|
| *T*[K] | 275 | | 298 | | 222 | | 255 | | 300 | | 330 | |
| | surf[c] | sub[c] | surf | sub | surf | sub | surf | sub | surf | sub | surf | sub |
| H | 1 | | 2 | | | | | | 1 | | 2 | |
| HH | | | | | | | | | 2 | | 2 | 1 |
| O | 2 | | 2 | 1 | | | 1 | | 2 | 1 | 3 | 1 |
| OH | 22 | 5 | 24 | 8 | 9 | 1 | 18 | 4 | 19 | 7 | 20 | 10 |
| OHH[d] | 21 | 13 | 21 | 16 | 23 | 7 | 24 | 14 | 23 | 20 | 23 | 20 |
| OO | 1 | | 1 | 1 | | | 1 | | 1 | 1 | 1 | 1 |
| OOH | 16 | 11 | 18 | 14 | 14 | 5 | 16 | 10 | 17 | 13 | 17 | 15 |
| OOHH | 35 | 63 | 30 | 53 | 52 | 81 | 37 | 65 | 31 | 49 | 29 | 43 |
| OOOHH | | 2 | 0 | 2 | | | | | | | | |
| av[e] | 3.07 | 3.68 | 3.00 | 3.54 | 3.44 | 3.91 | 3.18 | 3.74 | 3.06 | 3.55 | 3.02 | 3.42 |

[a] Abundances less than 1% were not included. [b] For the present model parameters, the melting point of the slab is 221 K for TIP4P and around 240 K (within several degrees) for EMP. [c] The surface and the subsurface layers were chosen to be 5 Å thick. The surface layer corresponds to the range of increase in molecular density. The subsurface layer directly adjacent to it corresponds to approximately constant density and includes ~85 molecules. The results are an average over the top and bottom slab surfaces. [d] Notation such as OHH means "one H-bond via O-atom of an $H_2O$ molecule, and two H-bonds via H-atoms". [e] Average coordination.

**Calculations of Vibrational Spectra: Technical Details.** Vibrational OH-stretch spectra were calculated using a scheme devised by us in the past and applied quite successfully for solid $H_2O$ systems.[24,26,27] OH bonds are treated as coupled local Morse oscillators. Vibrationally excited states describing OH-stretch motion are expanded in the exciton basis, $\sum c_i|1_i\rangle$, where $|1_i\rangle$ is a product basis state with one quantum in bond *i* and zero quanta in the remaining bonds. The OH bonds are coupled via intra- and intermolecular coupling; the latter is modeled as an oscillating dipole−dipole interaction. The influence of H-bonding on OH-stretch is modeled by assuming that the OH-bond frequency is a decreasing function $\omega(E_{||})$, where $E_{||}$ denotes the electric field component parallel to OH at the H-atom. $E_{||}$ is calculated as the field of the fixed charges and the induced dipoles of the EMP potential. This scheme was developed originally for solid water systems (clusters, surfaces, and ice) and was readjusted here for the treatment of the liquid. In solid systems, $E_{||}$ was calculated at a minimum structure or, in a more advanced version, averaged over intermolecular motion in the vicinity of the minimum.[24,29,30] The function $\omega(E_{||})$ was calibrated using select water clusters with known OH spectra and assignments,[24] and then applied to other systems. However, the liquid evolves continuously between different structures. One might consider an adiabatic approximation in which the spectra are calculated for a thermal distribution of instantaneous intermolecular configurations obtained in MD. However, past studies by other authors[31,32] indicate that thus-obtained spectra are too broad; that is, the intramolecular vibrations "feel" a force field which is averaged to some extent over fast intermolecular motions within an inherent structure ("motional narrowing"). In the present initial study, the electric field at each OH was simply averaged over a section of trajectory of 1 ps duration, on the order of a lifetime of an instantaneous hydrogen-bond network in water; the OH Hamiltonian was constructed accordingly and diagonalized to obtain the spectra. The spectra shown in panels (a) and (c) of Figure 1 are averages over spectra calculated for five consecutive 1 ps sections of the trajectory. The function $\omega(E_{||})$ was calibrated by performing a similar calculation on the cubic water octamer at 70 K. (The octamer spectrum was measured and assigned in the past, and spans the range ~3050−3700 $cm^{-1}$.[29]) The algorithm to calculate IR and Raman intensities for OH-stretch excitations is described in refs 24, 26, 27, and 30. The spectra were averaged over three perpendicular polarization directions. The spectra calculation was performed with EMP potential at 275 K, about 25 K above the slab melting point for this PES.

**Results for the Vibrational Spectra.** The results are shown in Figure 1; the experimental spectra of liquid water in panel (d) were taken from ref 31 (IR) and ref 33 (Raman). The IR and Raman spectra of the entire slab (panel (c)) are qualitatively consistent with experiment for bulk liquid water,[31,33−35] including the enhanced intensity of Raman with respect to IR in the low-frequency end of the spectral range. However, because of inaccuracies in the model, the Raman peak frequency is some 60 $cm^{-1}$ too high. The difference between the Raman and IR spectra was interpreted in the past as a residual of a much more dramatic effect observed in ice Ih,[34] for which the IR and parallel polarized Raman spectra look quite different; the ice IR band peaks at 3255 $cm^{-1}$, while the Raman spectrum is dominated by a relatively narrow feature at significantly lower frequency of 3150 $cm^{-1}$ (frequency values are given near the freezing point, as the spectra undergo substantial blueshift with increasing temperature[27,36,37]). The difference between the IR and Raman spectra stems from intermolecular coupling between OH-stretch vibrations. (Intramolecular coupling is also present but is small in condensed phases.[30]) This coupling results in collective OH-excitation modes with differing propensities for IR and Raman transitions. The ice Raman peak originates from the huge Raman intensity for the in-phase "breathing" oscillation of OH bonds. On the other hand, the ice IR peak originates from collective in-phase oscillations of the water dipoles, associated with the asymmetric stretch vibration. In the liquid and in amorphous ice, the influence of the coupling is reduced by a broad span of bond frequencies. However, the effect is by no means negligible, as evidenced, e.g., by a substantial difference between the measured Raman and infrared spectra and between vibrational spectra of $H_2O$ and HDO isotopically isolated in $D_2O$;[28,34] the presence of collective modes in amorphous ice was also demonstrated computationally.[28] In accord with these considerations, one can see in panel (c) significant differences between the calculated IR and Raman spectra and the densities of the excited states. Note that the IR spectra are influenced, in addition, by the increase in the bond dipole derivative with increasing frequency downshift.[24]

Panel (a) displays contributions to the different spectra from the two slab surfaces. The main difference versus panel (c) is enhanced contribution from the undercoordinated surface molecules. Distribution of bond frequencies for the different coordinations in the surface layers is shown in panel (b). The bond frequencies of the OHH molecules (with a dangling-O) appear in the range ~3550−3600 $cm^{-1}$, in accord with past studies of amorphous ice,[26] water clusters,[29] and ice nano-

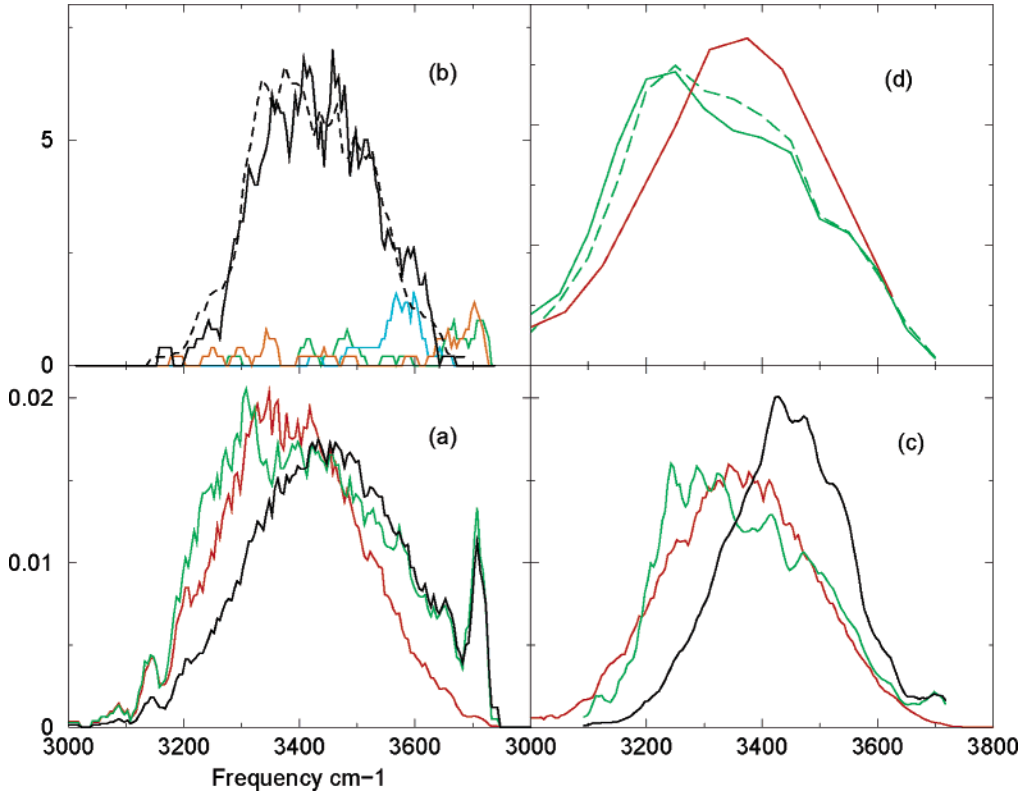


**Figure 1.** (a) OH-stretch spectrum of the surface layer. Contributions of 100 outermost molecules on both sides of the slab were included, corresponding to a layer thickness of about 7 Å on each side. Red, IR spectrum; green, parallel-polarized Raman; black, distribution of excited-state energies (with zero energy set at the ground vibrational state). (b) Density of bond frequencies for the different coordinations, in the surface layers. Black, OOHH; orange, OOH; cyan, OHH; green, OH. (c) OH-stretch spectrum of the entire 600-molecule slab, approximates the bulk liquid spectrum. Notation as in (a). Dotted black line, OOHH density for the entire slab ("bulk"). (d) Experimental spectra of liquid water. Red, IR, at 289 K; green, parallel-polarized Raman at 283 K (solid) and 303 K (dashed).

particles.[24] The dangling-OH of the OOH and OH molecules vibrate at ~3700 $cm^{-1}$. The frequencies of the "companion" hydrogen-bonded OH in the OOH molecules tend to appear in the low-frequency half of the OH band, while the "companion" frequencies of the two-coordinated OH molecules tend to be higher.

At the present stage, no effort has been made to reproduce the SFG spectra, which have been used extensively in the past to probe water surfaces.[1,4,5,11] Still, one may try some useful analysis based on the above results. In the SFG spectra, a spectral feature at 3700 $cm^{-1}$ originates undoubtedly from dangling-OH bonds. The bonded-OH band includes a broad feature at 3400 $cm^{-1}$ and a feature (or a shoulder) at ~3200 $cm^{-1}$; the relative intensities of the two features have been debated extensively. The 3400 $cm^{-1}$ feature has been reproduced consistently in a number of calculations of the SFG spectra, while the ~3200 $cm^{-1}$ one proved more elusive.[2,6−8,11] The latter feature was shown experimentally to be enhanced significantly for aqueous solutions of acids.[10] While the IR intensity is determined by the bond dipole derivative matrix element, and the Raman spectrum by the polarizability derivative, the SFG intensity includes both dipole and polarizability derivatives.[1,2,6,11] Thus, it appears reasonable to anticipate SFG features in the vicinity of Raman and/or IR maxima.

According to the calculations, the 3400 $cm^{-1}$ SFG peak coincides with a broad peak in the IR spectrum and overlaps with the low-frequency side of the peak in the density of states and in the density of frequencies of the four-coordinated molecules. Thus, the 3400 $cm^{-1}$ SFG feature appears to be dominated by OH-bond vibrations of four-coordinated surface molecules. The 3200 $cm^{-1}$ feature is suggested to originate from collective modes whose intensity is amplified with respect to the density of states. This feature is related to the low-frequency Raman feature observed for ice Ih and for liquid water (see panel (d) in Figure 1). In support of this point of view, one may note the enhanced Raman intensity below 3300 $cm^{-1}$ in panel (a) of Figure 1. Both the Raman and IR spectra in this range are clearly amplified with respect to the density of states. A typical excitation mode in this range is delocalized over a few bonds which happen to be particularly strongly H-bonded and which belong predominantly to four-coordinated molecules. These low-frequency modes tend to be characterized by a single dominant contribution ($\geq$50%) from one OH bond, but with significant in-phase contributions from another bond and smaller contributions from additional bonds. This modest delocalization is sufficient for the intensity amplification. One should emphasize that the effect is due predominantly to the intermolecular coupling (rather than intramolecular, as suggested in the past[5]); this conclusion is supported by the fact that, when the intermolecular coupling is set to zero, the excess low-frequency Raman and IR intensities disappear. Similarly, the low-frequency Raman peak of supercooled $H_2O$ was shown to be absent for HDO diluted in $D_2O$.[34] One may note that the intramolecular coupling in condensed $H_2O$ is expected to be small,[38] while the intermolecular coupling is enhanced for strongly H-bonded OH bonds.[24] Moreover, a significant intramolecular coupling effect would require both OH of an $H_2O$ to be strongly H-bonded, which appears unlikely. Since, in the low-frequency end of the spectrum, the intermolecular coupling generates collective modes of amplified intensity for both IR and Raman, one can reasonably expect an enhanced SFG signal as well. The fact that our calculations yield enhanced intensity at

$\sim$3200−3300 $cm^{-1}$, while the experimental SFG feature appears at 3200 $cm^{-1}$ or below, is consistent with the overestimation of the liquid Raman peak frequency in the present scheme (compare panels (c) and (d)).

**Acknowledgment.** J. P. Devlin, M. Shultz, P. Jungwirth, H. Allen, and D. Tobias are gratefully acknowledged for enlightening discussions. This research was funded by the Israel Science Foundation.

## References and Notes

(1) Du, Q.; Superfine, R.; Freysz, E.; Shen, Y. R. *Phys. Rev. Lett.* **1993**, *70*, 2313.

(2) Benjamin, I. *Phys. Rev. Lett.* **1994**, *73*, 2083.

(3) Dang, L. X.; Chang, T. M. *J. Chem. Phys.* **1997**, *106*, 8149.

(4) Shultz, M. J.; Baldelli, S.; Schnitzer, C.; Simonelli, D. *J. Phys. Chem. B* **2002**, *106*, 5313.

(5) Raymond, E. A.; Richmond, G. L. *J. Phys. Chem. B* **2004**, *108*, 5051.

(6) Morita, A.; Hynes, J. T. *J. Phys. Chem. B* **2002**, *106*, 673.

(7) Morita, A.; Hynes, J. T. *Chem. Phys.* **2000**, *258*, 371.

(8) Perry, A.; Ahlborn, H.; Space, B.; Moore, P. B. *J. Chem. Phys.* **2003**, *118*, 8411.

(9) Wilson, K. R.; Cavalleri, M.; Rude, B. S.; Schaller, R. D.; Nilsson, A.; Pettersson, L. G. M.; Goldman, N.; Catalano, T.; Bozek, J. D.; Saykally, R. J. *J. Phys.: Condens. Matter* **2002**, *14*, L221.

(10) Mucha, M.; Frigato, T.; Levering, L. M.; Allen, H. C.; Tobias, D. J.; Dang, L. X.; Jungwirth, P. *J. Phys. Chem. B* **2005**, *109*, 7617.

(11) Brown, E. C.; Mucha, M.; Jungwirth, P.; Tobias, D. J. *J. Phys. Chem. B* **2005**, *109*, 7934.

(12) Petersen, P. B.; Saykally, R. J. *J. Phys. Chem. B* **2005**, *109*, 7976.

(13) Jorgensen, W. L.; Chandrasekhar, J.; Madura, J. D.; Impey, R. W.; Klein, M. L. *J. Chem. Phys.* **1983**, *79*, 926.

(14) Sanz, E.; Vega, C.; Abascal, J. L. F.; MacDowell, L. G. *Phys. Rev. Lett.* **2004**, *121*, 1165.

(15) Buch, V.; Sandler, P.; Sadlej, J. *J. Phys. Chem. B* **1998**, *102*, 8641. EMP corresponds to a modified version of the potential described in the next reference.

(16) Kuwajima, S.; Warshel, A. *J. Phys. Chem.* **1990**, *94*, 460.

(17) Ryckaert, J. P.; Ciccotti, G.; Berendsen, H. J. C. *J. Comput. Phys.* **1977**, *23*, 327.

(18) Allen, M. P.; Tildeslay, D. J. *Computer Simulations of Liquids*; Oxford Science Publications: Oxford, 1993; Chapter 5.

(19) Valleau, J. P.; Whittington, S. G. In *Statistical Mechanics A: Modern Theoretical Chemistry*; Berne, B. J., Ed.; Plenum: New York, 1977; Vol. 5, pp 137−168.

(20) In studies of condensed-phase systems made of molecules with large dipoles, treatment of long-range forces may require particular attention in calculations of some of the properties.[18,19] The problem is that the dipole−dipole interaction decays as $r^{-3}$, while in a three-dimensional system, the number of dipoles at a distance between $r$ and $r + dr$ increases as $r^2$; thus, the effective decay rate of the interaction is very slow ($r^{-1}$). However, this difficulty is less serious in the case of two-dimensional systems, since the number of dipoles increases with distance only as $r$, and therefore, the interaction decays, effectively, as $r^{-2}$. One may note that use of the commonly employed Ewald summation in surface studies employing slabs is problematic, e.g., Ewald summation imposes parallel dipoles in adjacent boxes, while in the physical reality, the dipoles will tend to cancel. The problem was discussed in ref 19.

(21) Buch, V.; Devlin, J. P. *J. Chem. Phys.* **1991**, *94*, 4091.

(22) Buch, V. *J. Chem. Phys.* **1992**, *96*, 3814.

(23) Buch, V. *J. Chem. Phys.* **1990**, *93*, 2631.

(24) Buch, V.; Baurecker, S.; Devlin, J. P.; Buck, U.; Kazimirski, J. *Int. Rev. Phys. Chem.* **2004**, *23*, 375, and unpublished calculations by the author on models described in this reference.

(25) Kroes, G. *J. Surf. Sci.* **1992**, *275*, 365.

(26) Rowland, B.; Kadagathur, S.; Devlin, J. P.; Buch, V.; Feldmann, T.; Wojcik, M. *J. Chem. Phys.* **1995**, *102*, 8328.

(27) Buch, V.; Devlin, J. P. *J. Chem. Phys.* **1999**, *110*, 3437.

(28) Wojcik, M. J.; Buch, V.; Devlin, J. P. *J. Chem. Phys.* **1993**, *99*, 2332.

(29) Buck, U.; Ettischer, I.; Melzer, M.; Buch, V.; Sadlej, J. *Phys. Rev. Lett.* **1998**, *80*, 2578.

(30) Sadlej, J.; Buch, V.; Kazimirski, J. K.; Buck, U. *J. Phys. Chem. B* **1999**, *103*, 4933.

(31) Rice, S. A.; Bergren, M. S.; Belch, A. C.; Nielson, G. *J. Phys. Chem.* **1983**, *87*, 4295. Belch, A. C.; Rice, S. A. *J. Chem. Phys.* **1983**, *78*, 4817; *87*, 4295.

(32) Ojamae, L.; Tegenfeldt, J.; Lindgren, J.; Hermansson, K. *Chem. Phys. Lett.* **1992**, *195*, 97.

(33) Scherer, J. R.; Go, M. K.; Kint, S. *J. Chem. Phys.* **1974**, *78*, 1304.

(34) Hare, D. E.; Sorensen, C. M. *J. Chem. Phys.* **1992**, *96*, 13.

(35) Green, J. L.; Lacey, A. R.; Sceats, M. G. *J. Phys. Chem.* **1986**, *90*, 3958.

(36) Scherer, J. R.; Snyder, R. G. *J. Chem. Phys.* **1977**, *67*, 4794.

(37) Clapp, M. L.; Miller, R. E.; Worsnop, D. R. *J. Phys. Chem.* **1995**, *99*, 6317.

(38) Low intramolecular coupling can be inferred from the modest symmetric−asymmmetric stretch splitting of $H_2O$ in the water octamer: 24−30 $cm^{-1}$, as compared to 110 $cm^{-1}$ for gaseous $H_2O$.[30] A similarly small splitting of 45 $cm^{-1}$ was measured for $H_2O$ molecules isolated in $D_2O$ ice; see Devlin, J. P. *Int. Rev. Phys. Chem.* **1990**, *9*, 29.